

ANALYTICAL SIMULATION OF EARTHQUAKE DAMAGE OF WALL-TYPE PIERS

MOHAMMAD REZA SALAMY¹, JUNICHI SAKAI², SHIGEKI UNJOH³

¹Member of JSCE, Dr. of Eng., Public Works Research Institute, Earthquake Engineering Research Team
Earthquake Disaster Prevention Research Group, Minamihara 1-6, Tsukuba-shi, Japan 305-8516

²Member of JSCE, Dr. of Eng., Public Works Research Institute, Earthquake Engineering Research Team

³Member of JSCE, Dr. of Eng., Public Works Research Institute, Leader of Earthquake Engineering Research Team

1. Introduction

Damage to a pre-stressed concrete bridge during Niigata-Chuetsu 2004 earthquake is simulated in this paper by means of nonlinear finite element method. Predicted crack pattern during the analysis procedure is utilized to estimate maximum displacement the bridge perhaps experienced during the earthquake. The bridge is supported by two pre-stressed concrete side walls and two main RC wall-type piers with simple connection in order to eliminate moment transformation from piers to the bridge deck and foundation. There are plenty of studies on these types of piers in laboratory level but this particular case provided a unique opportunity to examine those theories and put them in practice. Two dimensional finite element method is employed to model those piers under cyclic and monotonic loads to estimate structure situation after the earthquake. By comparing extreme values of cyclic response with that of monotonic it is found that both responses are very similar since

deterioration of load capacity under cyclic load is not significant. Therefore static analysis is supposed to be enough in this stage to evaluate pier behavior during the earthquake though more detailed simulation under real earthquake load is authors' interest for future works on this case.

Application of the presented finite element method to predict response of the piers is verified in previous studies on deep beam behavior¹. Since load-deflection responses of the piers are unknown, crack pattern is utilized to predict level of load and deflection those members might have experienced. Thereafter, residual strength and ductility of the bridge from current damage state is investigated.

As for analytical simulation by finite element method, the constitutive behavior of concrete is represented by a smeared crack model with two dimensional concrete elements. Two main crack models, fixed and rotating crack models, are tried in preliminary analysis. In both cases flexural failure is detected. It is known, however,

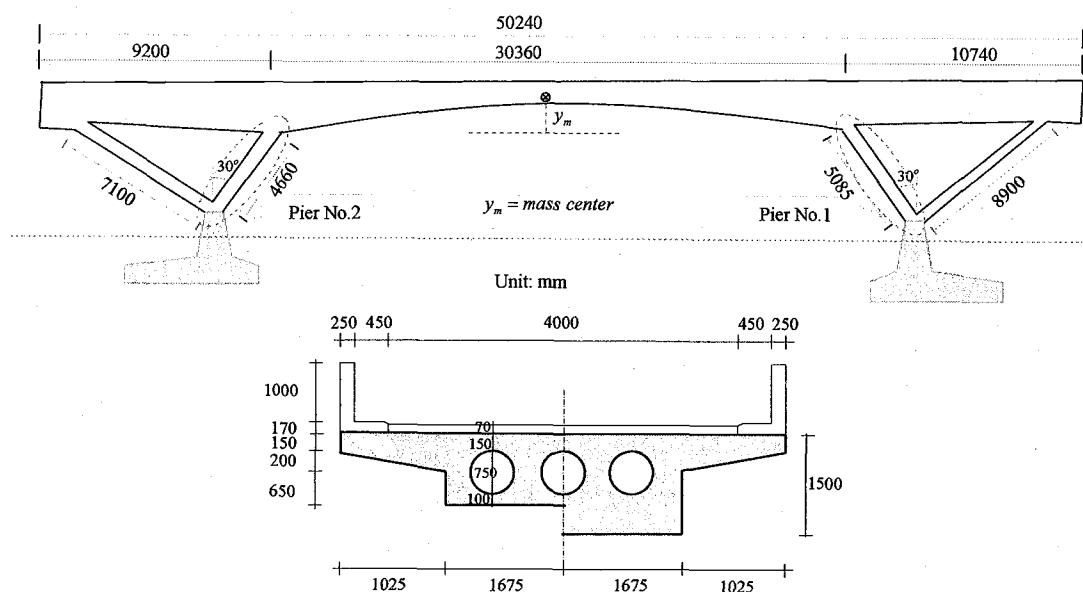


Fig.1. Bridge geometry and section detail

that fixed crack model predict actual crack pattern more realistic and robust than that of rotating crack model. Due to the methodology applied here based on crack pattern evaluation, fixed crack model is employed for investigation.

2. Geometry properties and FE modeling

An overpass bridge with a total length of 50.3m and width of 5.4m shown in Fig.1 is investigated here to assess damage level resulted from 2004 Niigata-Chuetsu earthquake. Super-structure consists of a pre-stressed hollow deck with variable depth. Wall-type piers are supporting bridge deck and connected to the deck and foundations by longitudinal pines which imply no moment shall be transferred through the connecting joints. Investigated wall-piers are indicated by Pier No.1 and 2 in Fig.1 with a constant thickness of 400 mm. It is, however, noted that thickness of top and bottom of each wall is reduced to 150 mm to ensure pin connection between two components. To achieve better accuracy, those parts are modeled by finite element as interface elements (only connection between foundation and walls) with identical thickness to that of actual joint. In numerical simulation dead load affected on wall piers is calculated by assuming that all dead loads are divided identically between only these piers, which this assumption is believed to have enough accuracy due to the pre-stressing force effect on side walls. On the other hand lateral load subjected to super-structure mass center is calculated by taking into account effect of walls dead weights in subjected lateral load. Bridge geometry is shown in Fig.1.

In order to distribute lateral load on wall-piers; linear spring model is applied by means of un-cracked section as illustrated in Fig.2. Generalize potential energy concept is utilized to solve the equation system and find unknown values Δ and θ . Generalize potential energy Π_p is then written as:

$$\Pi_p = \frac{1}{2} K_1 \Delta^2 + \frac{1}{2} K_2 (\Delta + \theta \ell_1)^2 + \frac{1}{2} K_3 (\Delta + (\ell - \ell_2) \theta)^2 + \frac{1}{2} K_4 (\Delta + \theta \ell)^2 - P(\Delta + \frac{\ell}{2} \theta) \quad (1)$$

For any admissible set of infinitesimal displacement $\{\delta D_i\}$ where in $i=1, 2, 3, \dots, n$ we will have:

$$\frac{\partial \Pi_p}{\partial D_i} = 0 \quad (2)$$

therefore $\frac{\partial \Pi_p}{\partial \Delta} = 0$ and $\frac{\partial \Pi_p}{\partial \theta} = 0$ leads to the following matrix equation.

$$\begin{bmatrix} K_1 + K_2 + K_3 + K_4 & K_2 \ell_1 + K_3 (\ell - \ell_2) + K_4 \ell \\ \text{Sym.} & K_2 \ell_1^2 + K_3 (\ell - \ell_2)^2 + K_4 \ell^2 \end{bmatrix} \begin{bmatrix} \Delta \\ \theta \end{bmatrix} = \begin{bmatrix} P \\ \frac{P\ell}{2} \end{bmatrix} \quad (3)$$

After some algebra, distributed lateral load of each wall will be found as

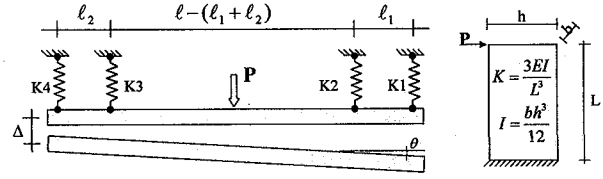


Fig.2. Lateral load distribution on walls with simplified linear spring model

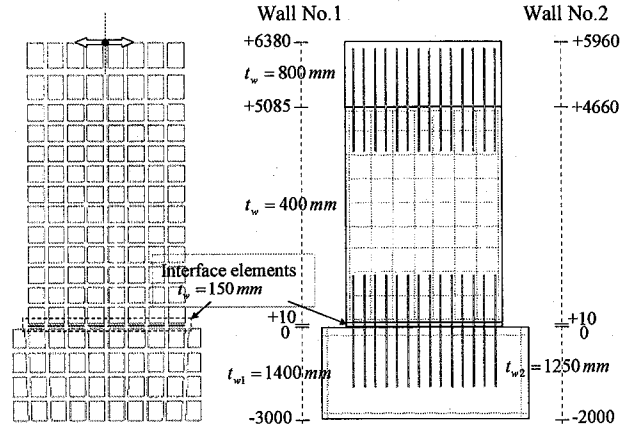


Fig.3. Mesh discretization (left) and reinforcement arrangement and geometry in different level (right)

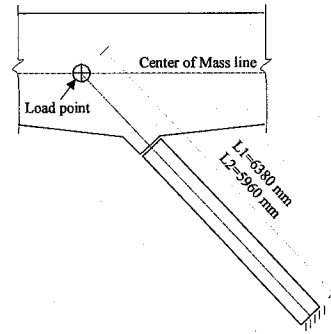


Fig.4. Loading point

$\{F_1 = 0.10P, F_2 = 0.43P, F_3 = 0.36P, F_4 = 0.11P\}$ where in only forces F_2 and F_3 , relevant to wall-piers No.1 and 2, are considered.

On the other hand, in order to calculate actual point of the affected loads on the walls, mass center of superstructure is determined. After some algebra mass center y_m , which implies level of subjected lateral load, as distance from the lowest part of the deck (Fig.1) is found as:

$$y_m = 1115 \text{ mm} \quad (4)$$

Total height of each wall is also defined by means of this value as well as inclination angle (Fig.3 and 4).

Fig.3 shows the employed mesh discretization in finite element analysis along with geometry of walls and

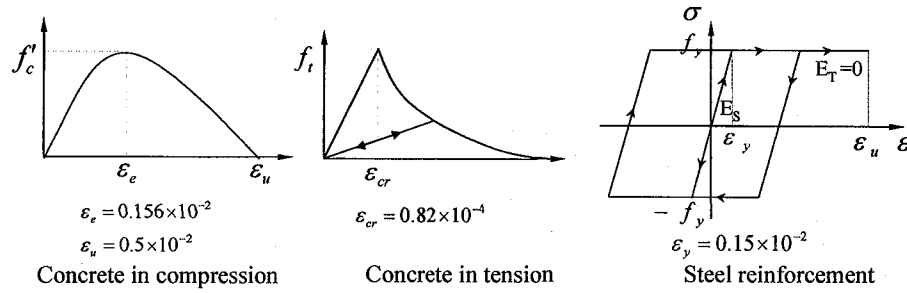


Fig.5. Concrete and steel material models

reinforcement arrangement. In finite element simulation, constitutive behavior of concrete is represented by a smeared crack model, which in the damaged material is still continuum. Preliminary analyses were conducted by means of rotating crack model and fixed crack model. Due to those results it is found that shear is not a dominant problem and most possibly, failure will occur in flexural mode. Displacement-control with regular Newton-Raphson solution technique is adopted to solve equilibrium equations. The method, however, yielded robust load-deflection response with almost no diverged steps during solution procedure. All elements are 2D elements in plane-stress condition while due to sudden change of width in adjacent of wall and foundation to produce hinge connection, interface element is employed for this portion.

Concrete material models in tension and compression are Hordijk² and Feenstra³ models respectively. Concept of compression field theory⁴ is also employed in analysis throughout. Application of aforementioned models is reported elsewhere¹. Steel reinforcements on the other hand are modeled as a cyclic elastic-perfect plastic material with no hardening after yield point. All reinforcements are smeared out over concrete elements with relevant thickness in each direction. No bar element, therefore, is modeled for this analysis which implies perfect bond assumption will be inevitable. Applied constitutive models for concrete and steel are schematically illustrated in Fig. 5. As mentioned since

shear has no dominant influence on failure mode, fixed crack model produced better prediction in terms of stable crack direction as well as more load cycles could be induced into the structures. The results presented hereafter are based on fixed crack model. Bond-slide is neglected and perfect connection between steel and concrete is assumed since all reinforcements are smeared out over each finite element. Concrete compressive stress $f'_c = 35 \text{ MPa}$, modulus of elasticity $E_c = 30 \text{ GPa}$ and steel yield stress and modulus of elasticity is assumed $f_y = 300 \text{ MPa}$ and $E_s = 200 \text{ GPa}$ respectively. Other properties such as tensile stress and fracture energies of concrete are calculated by means of JRA code (Japan Road Association)⁵ recommendations. Released fracture energy during cracking process is taken into account in the analyses to ensure accuracy and objectiveness of finite element simulation in terms of the applied mesh size.

3. Load-deflection response of walls

Fig.6 shows analytical results of wall No.1 and 2 respectively. Both cyclic and monotonic responses are illustrated in each figure. Despite previous experiences¹ which in usually fixed crack model resulted premature failure while dealing with shear issue, here no difficulties such as divergence of solution process as well as sudden drop in load-deflection response has been signaled since flexural behavior dominated overall failure mode. A comparison between monotonic and cyclic response

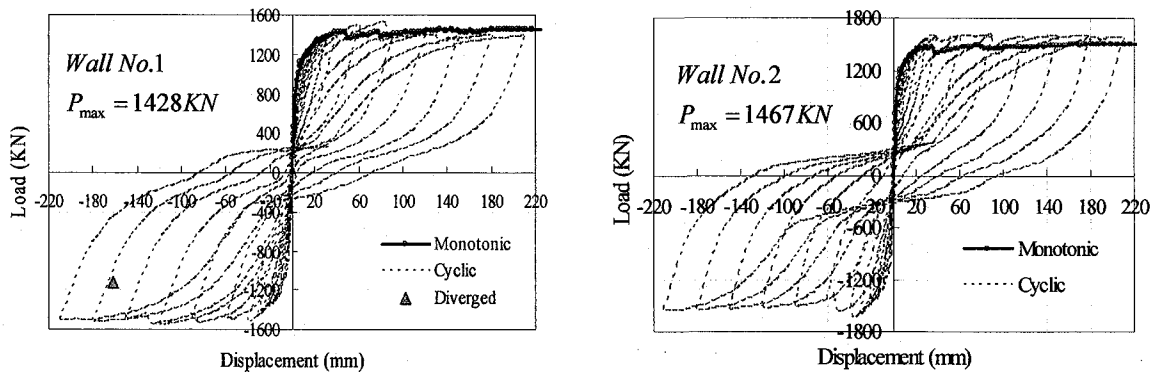


Fig.6. Monotonic and Cyclic response on wall No.1 and No.2

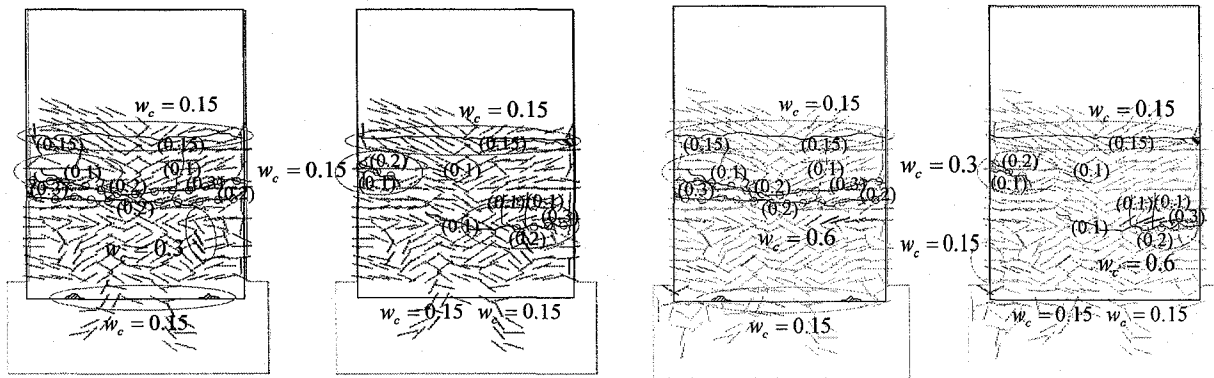


Fig.7. Prediction crack patterns at cycles δ_1 (two left) and δ_2 (two right) after unloading versus surveyed crack patterns

indicates small deterioration of load capacity in latter case during further load cycles. It is noted, however, that load capacity was expected to receive more deterioration by increasing of load cycles. This implies that member's stiffness is not decreasing and spurious stiffness exists in some part of numerical simulation. This phenomenon can be attributed to the fixed representation of cracks which results higher stiffness due to constraining of cracks' directions once crack developed within an element. In these figures full deformation capacities of the walls are depicted while, as it will be discussed later, current situation of the structures based on the present results experienced far less deformation. Full capacity in analysis means the point where numerical iterations fail to converge to the exact solution. In other word, last load increments are dubious due to chronic divergence of iterative solution. However, the results are probably a good prediction of real structure response.

4. Crack patterns of wall No.2 under cyclic load

Crack patterns in two stages of load cycles, depicted in Fig.7 are shown and discussed in this section. Each load cycle consists of four load step, where in crack pattern can be drawn, are maximum load of each cycle in

positive direction, return to zero load (called here unloaded stage), reverse cycle in negative direction, return to zero load. Extreme values of each load cycle have the largest crack width whereas cracks in totally exhausted load condition have smallest width and implies residual cracks which are remaining unclosed. It should be noted here that since in employed crack model secant modulus is adopted to model unloading process, except fully opened cracks, other cracks will be closed after the applied load is eliminated unless steel reinforcements yielded already or residual displacement in piers is developed. Crack width is not usually a direct output of finite element codes and in most cases is represented by strain in integration points. Here output strains are translated into the crack width for the sake of comparison with observed cracks of the piers. Crack width w_c can be expressed by following equation.

$$w_c = \varepsilon_{cr} \cdot h \quad (5)$$

wherein ε_{cr} is crack strain and h is crack bandwidth (element characteristic length parameter used for released fracture energy calculation) and estimated for nonlinear finite elements as $h = \sqrt{A}$ where in A is element total area. In order to compare analytically obtained crack width with that of surveyed ones, we may follow two scenarios as, first to assign crack width of extremes load of a certain cycle, second to compare residual cracks of analysis after complete elimination of lateral load of each cycle. The later scenario is believed to be more realistic situation of the structure since lateral load is already eliminated therefore this case is merely examined and discussed hereafter.

The methodology employed here to assess load and displacement level where the structure possibly experienced is to pick up predicted crack width which fits best to the actual situation of structure. Fig.7 shows crack patterns of two cycles load indicated in Fig.8 by δ_1 and δ_2 after lateral loads are totally exhausted. It is clear that numerical simulation has only one crack pattern for each

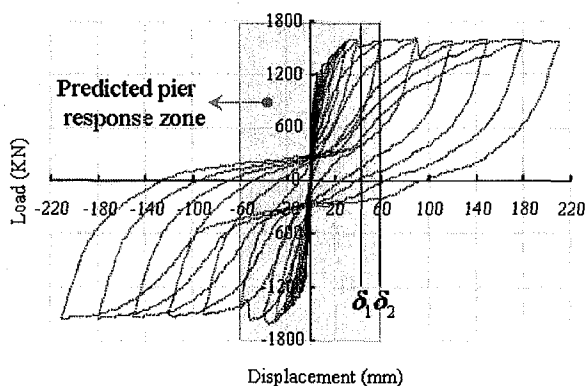


Fig.8. Investigated load steps of each cycle

case which is compared with two faces of the cracked wall since real structure experienced three dimensional load condition therefore cracks of two faces are not similar. Crack widths indicated by w_c are those of analyses while observed crack widths are presented in parentheses. Some parts have been severely damaged which may represent spalling off the concrete in those areas. Since the finite element method used for this investigation is not supporting discrete elements, spalling or crushing of concrete in crucial regions can not be directly obtained from the results. Therefore, strain in each portion is the only way to assess state of concrete and evaluate if the concrete is already crushed or not. This method is utilized here to look into the concrete and determine state of stress and strain in target point by means of applied constitutive model for concrete in compression (Fig.5 left).

Figure 9 illustrates principal strain of the wall in cycle δ_1 after the pier is unloaded and lateral load is totally eliminated. Minimum principal strain here represents mainly compressive strain. Since the pier is subjected to reverse cycles, both sides are under a sequence of tension and compression. Therefore we can see crack opening in both sides while under compression, strain is accumulated and those parts are deformed. The figure clearly shows opening of cracks or complete separation of two parts, which is a result of using interface element, after total fracture energy release as well as localized compressive plastic deformation. In this portion concrete strain goes beyond concrete ultimate strain either in tension or compression. This phenomenon, although can be considered as spalling of the concrete itself particularly in case of compressive failure, but at least represents deteriorated of concrete in this part by means of inactive cracks where in no interaction between stress and strain is maintained. It is very important to note again that all strains drawn in this figure are residual strain which in applied load is almost exhausted.

Shaded area in Fig.8 is most possibly the zone which the wall has experienced during the earthquake due to the aforementioned reasons. Area between $\delta_1 = 40\text{ mm}$ and $\delta_2 = 60\text{ mm}$ shows the maximum deflection the wall has received where in crack patterns are also presented in these two limits.

To investigate behavior of the wall during the earthquake, monotonic and extreme values of load cycles with sequence of events are depicted in Fig.10. In this figure different stages of steel and concrete states are illustrated. Tensile reinforcement in cut off area, where in reinforcement area is reduced, is yielded as early as in 3.5 mm of displacement and consequently peak load at $\delta = 28.5\text{ mm}$ is obtained. During the entire analysis process no reinforcement is yielded the adjacent of footing and the wall in tension. In $\delta = 41.5\text{ mm}$ reinforcements are yielded in compression. Following compressive yielding of rebar, concrete spalled in $\delta = 59.5\text{ mm}$ almost in same level as δ_2 cycle. It is noted, however, that in real damage survey, spalling of concrete is observed in almost same location as analysis

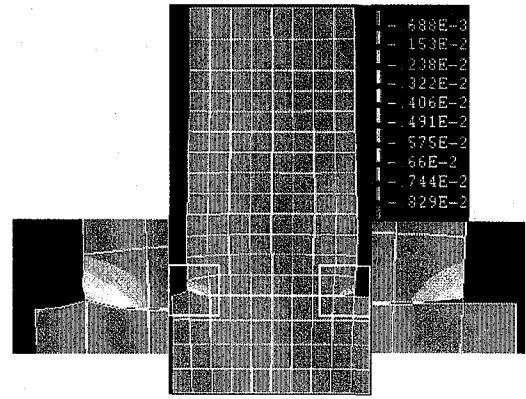


Fig.9. Minimum principal strain in cycle δ_1 after unloading

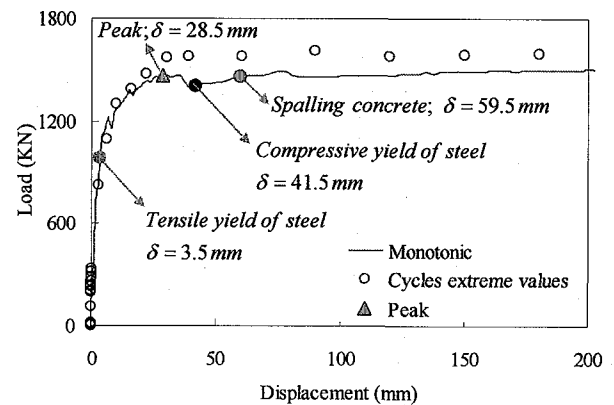


Fig.10. Predicted steel and concrete state

anticipated. Predicted response shows a deflection between 40 mm to 60 mm which in average we may say $\delta = 50\text{ mm}$ is an acceptable estimation. It can be seen from Fig.8 that the wall still reserves a large capacity of deformation as far as 200 mm. This capacity of deformation implies that the pier response was in acceptable range and ductility of the pier is preserved. Therefore bridge is in safe side and application of conventional form of repair to strengthen the structure against similar earthquake is acceptable.

5. Stress distribution of steel reinforcements

It is shown in Fig.10 that steel reinforcements yield at about half of the maximum load capacity of the pier at about 3.5 mm of deflection. Stress in steel reinforcement is investigated in this section and drawn in Fig.11. Steel mesh of the wall in vertical direction yields in tension as near the peak load of second cycle with a relative load of 980 KN just before the peak load of this cycle which is 1100 KN. It is almost clear that if the state of structure response is considered to reach to the further cycles, plastic strain will be developed in some part of the wall. Patterns of development of plastic strain due to yielding of steels are presented in Fig.11. Although main

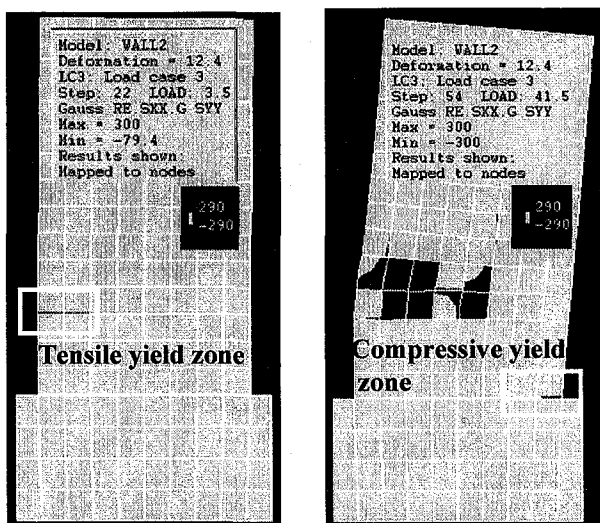


Fig.11. Stress contours and yielding zone of reinforcement in tension (left) and compression (right)

reinforcement in compression have been almost in elastic range but some parts are yielded in compression as shown in right side picture (small selected area) of Reinforcement yielded in tension is shown in the left picture of Fig.11. Section where in reinforcements are cut off developed first yielding portion in tension therefore in similar structures similar behavior is expected. In actual situation also cracks occurred in almost same location which agrees well with those predicted by analysis.

6. Conclusion

A pre-stressed concrete bridge with RC wall-type piers which was damaged during Niigata-Chuetsu 2004 earthquake is investigated in this paper to assess damage level by means of nonlinear finite element method. For the sake of simplicity, equivalent cyclic load applied to estimate dynamic loading condition which the bridge experienced during the earthquake. The method yielded reasonable results in terms of load-displacements response as well as crack patterns and steel stress and strain state which both play crucial role for damage assessment of structures. Crack pattern of each cycles are compared and evaluated with surveyed crack patterns to select the best fit to the current situation of the investigated piers. Through this methodology level of load and deformation the pier possibly experienced during the earthquake is determined. It is found that despite yielding of steel at early stage and compressive failure of concrete in some part of the wall, there still remains a rather large deformation capacity which in safety of the bridge is ensured. Therefore conventional method for repair can be applied to this structure. Since the bridge is located in very active earthquake region, three dimensional dynamic analysis under real earthquake load is authors' interest for further investigation to ensure safety and performance of the structure for future earthquakes.

ACKNOWLEDGEMENT

Bridge data and structural details are provided by and Mr. Daizo Maruyama who is Sub-Leader of Maintenance Group at Niigata Branch of East Nippon Expressway Company Limited. His kind help is gratefully acknowledged.

REFERENCES

1. Salamy M. R., Kobayashi H. and Unjoh S.; Experimental and analytical study on RC deep beams, *Asian Journal of Civil Engineering (AJCE)*, Vol.6, No.5, pp.409-422, November 2005.
2. Hordijk, D.A., *Local approach to fatigue of concrete*, PhD thesis, Delft University of Technology, 1991.
3. Feenstra, P.H., "Computation aspects of biaxial stress in plain and reinforced concrete", PhD thesis, Delft University of Technology, 1993.
4. Vecchio, F. and Collins, M.P., *The modified compression field theory for reinforced concrete elements subjected to shear*, *ACI structural journal*, V.3, No.4, 1986, pp. 219-231
5. Japan Road Association. *Design specifications of highway bridges. Part V: seismic design*; (in Japanese), 2002.